Available online at www.sciencedirect.com
ScienceDirect
International Journal of Heat and Mass Transfer 50 (2007) 1097–1105
International Journal of HEAT and MASS TRANSFER
www.elsevier.com/locate/ijhmt

The effect of wall conduction for the extended Graetz problem for laminar and turbulent channel flows

B. Weigand [a,*], G. Gassner [b]

[a] Institut für Thermodynamik der Luft- und Raumfahrt, Universität Stuttgart, Pfaffenwaldring 31, 70569 Stuttgart, Germany
[b] Institut für Aero-und Gasdynamik, Universität Stuttgart, Pfaffenwaldring 21, 70569 Stuttgart, Germany

Received 29 November 2005; received in revised form 23 June 2006
Available online 30 October 2006

Abstract

Axial heat conduction effects within the fluid can be important for duct flows if either the Prandtl number is relatively low (liquid metals) or if the dimensions of the duct are small (micro heat exchanger). In addition, axial heat conduction effects in the wall of the duct might be of importance. The present paper shows an entirely analytical solution to the extended Graetz problem including wall conduction (conjugate extended Graetz problem). The solution is based on a selfadjoint formalism resulting from a decomposition of the convective diffusion equation into a pair of first order partial differential equations. The obtained analytical solution is relatively simple to compute and valid for all Péclet numbers. The analytical results are compared to own numerical calculations with FLUENT and good agreement is found.
© 2006 Elsevier Ltd. All rights reserved.

1. Introduction

The prediction of the heat transfer characteristics in pipe and channel flows is of theoretical interest and practical importance. Heat transfer of hydrodynamically fully developed pipe and channel flows has therefore attracted a lot of researchers in the past. Normally, the effect of streamwise conduction in the flow on the heat transfer can be neglected. The classical Graetz problem deals with heat transfer in the thermal developing region of the flow under such conditions. Good reviews on this subject for laminar and turbulent duct flows can be found in [1,2]. However, if the Péclet number ($Pe_D = Re_D Pr$) in the flow is small, axial heat conduction in the fluid becomes important. This is the case, for example, in compact heat exchangers where liquid metals are used as the working fluids or in micro heat exchangers, where the overall dimensions are very small. In the past, many investigations have been carried out which dealt with the solution of the extended Graetz problem (the Graetz problem considering axial heat conduction in the fluid) for thermally developing laminar flow in a pipe or in a parallel plate channel. Extensive literature reviews on this subject are given in [1,3]. Many of the solutions cited in [1,3] for the extended Graetz problem are based on the fundamental assumption that the solution of the problem has the same form of the series solution as the Graetz problem without axial heat conduction in the fluid. This approach results in a non-selfadjoint eigenvalue problem with eigenvalues that could, at least in principle, be complex and eigenvectors that could be incomplete. Several strategies have been developed in the past to overcome this problem. Hsu [4], for example, constructed the solution of the problem from two independent series solutions for $x < 0$ and $x > 0$. Both the temperature distribution and the temperature gradient were then matched at $x = 0$ by constructing a pair of orthonormal functions from the non-orthogonal eigenfunctions by using the Gram–Schmidt-orthonormalization procedure. Hence this method is clearly plagued with the uncertainties arising from an expansion in terms of eigenfunctions and eigenvalues belonging to a non-selfadjoint

* Corresponding author. Tel.: +49 711 685 3590; fax: +49 711 685 2317.
E-mail address: bw@itlr.uni-stuttgart.de (B. Weigand).

0017-9310/$ - see front matter © 2006 Elsevier Ltd. All rights reserved.
doi:10.1016/j.ijheatmasstransfer.2006.06.047

Nomenclature

a	thermal diffusivity (m^2/s)
c_p	specific heat at constant pressure (J/(kg K))
D	hydraulic diameter, $D = 4h$ (m)
d	wall thickness (m)
$\vec{f}$, $\vec{S}$	vectors (–)
h	distance between centreline and wall (m)
k	thermal conductivity (W/(mK))
L	matrix operator (–)
$\tilde{l}_1$	half length of the heated zone (m)
Nu_D	Nusselt number based on the hydraulic diameter (–)
Pr	Prandtl number (–)
Pe_h, Pe_D	Péclet number based on h and D (–)
Pr_t	turbulent Prandtl number (–)
Re_h, Re_D	Reynolds number based on h and D (–)
T	temperature (K)
T_0	uniform temperature for $x \to -\infty$ (K)
T_1	elevated outer wall temperature for $-l_1 < x < l_1$ (K)
T_b	bulk-temperature (K)
u	axial velocity (m/s)
$\overline{u}_0$	axial mean velocity (m/s)
x, y	coordinates (m)

Greek symbols

ε_{hx}, ε_{hy}	eddy diffusivity (m^2/s)
ε_m	eddy kinematic viscosity (m^2/s)
ρ	density (kg/m^3)
λ_j	eigenvalue (–)
Θ	dimensionless temperature (–)
ν	kinematic viscosity (m^2/s)
Σ	axial energy flow (–)
$\vec{\Phi}_j$	eigenfunction (–)

operator. However, Papoutsakis et al. [5] showed that it is possible to produce an entirely analytical solution to the extended Graetz problem for Dirichlet boundary conditions. Their solution is based on a selfadjoint formalism resulting from a decomposition of the convective diffusion equation into a pair of first order partial differential equations. In addition, several investigations have been carried out in the past concerning the extended Graetz problem in a parallel plate channel. Deavours [6] presented an analytical solution for the extended Graetz problem by decomposing the eigenvalue problem for the parallel plate channel into a system of ordinary differential equations for which he proved the orthogonality of the eigenfunctions. There are also several numerical investigations which deal with the extended Graetz problem for laminar flow in a pipe or a parallel plate channel, see [1–3]. Axial heat conduction might also be important for turbulent internal flows, if the Prandtl number is sufficiently small. Lee [7] studied the extended Graetz problem in turbulent pipe flow. He found that for Péclet numbers below 100, axial heat conduction in the fluid becomes important in the thermal entrance region. Lee used the method of Hsu [4] to obtain a series solution for the problem. Weigand [8] extended the method of Papoutsakis et al. [5] to solve the extended Graetz problem for turbulent flow inside a pipe and a parallel plate channel. Weigand et al. [9] investigated numerically the extended Graetz problem in a parallel plate channel with piecewise constant wall temperature boundary conditions. They used different turbulence models for calculating the turbulent heat flux. Their investigation showed that the normally used assumption that the eddy diffusivity in axial and normal direction is the same is correct for the range of parameters under investigation. The effect of a piecewise changing wall heat flux or wall temperature has been analytically studied by Weigand et al. [10] and Weigand and Lauffer [11]. Despite the large amount of work, which has been done on the extended Graetz problem for laminar and turbulent duct flows, very little investigations are known which study analytically the effect of conduction in the wall on the heat transfer in a duct. This is because of the difficulties, which are present in this case, to develop an analytical solution for the problem. Studies by Mori et al. [12,13] and by Guedes and Özisik [14] for example have taken into account axial conduction in the wall, but not in the fluid. A work by Yin and Bau [15] considered axial heat conduction in the wall as well as in the fluid for a laminar flow in a parallel plate channel. A complicated analysis has been presented, where an infinite set of algebraic equations had to be solved. In addition, the above mentioned paper used a boundary condition at the position where the jump in the outer wall temperature occurred. The constants in the solution were then computed in the sense of weighted residuals. As it is well known, it is highly questionable to prescribe this sort of inlet boundary condition for the extended Greatz problem (see also Weigand [3]). Studies, dealing with the analytical solution of the extended Graetz problem considering axial heat conduction in the wall for turbulent internal flows are not known to the best knowledge of the authors. The purpose of the present paper is to investigate analytically the extended Graetz problem for laminar and turbulent flow in a parallel plate channel including axial heat conduction in the solid. The analytical solution here presented will not be plagued with the uncertainties arising from an expansion in terms of eigenfunctions and eigenvalues belonging to a non-selfadjoint operator. Furthermore, the solution for the "complete area" ($-\infty < x < \infty$) will be presented. Thus, the temperature field at $x = 0$ is part of the solution and not a boundary condition.

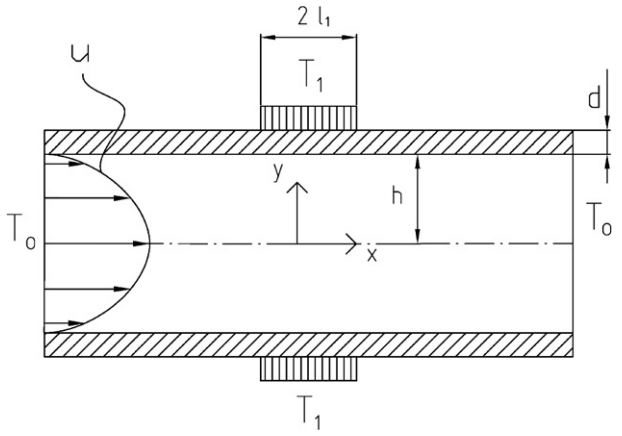

Fig. 1. Geometrical configuration and coordinate system.

2. Analysis

Fig. 1 shows the geometrical configuration and the coordinate system. The characteristic length h denotes half of the channel height. It is assumed that the flow enters the duct with a hydrodynamically fully-developed laminar or turbulent velocity profile and with a uniform temperature profile for $x \to -\infty$. The outer wall temperature is maintained at T_0 for $x < -l_1$ and for $x > +l_1$ and at T_1 for $-l_1 \leqslant x \leqslant l_1$. The wall thickness is denoted by d. For $x \to +\infty$ the temperature attains again the uniform temperature T_0. In order to obtain the temperature distribution within the solid layer and within the fluid, the energy equation has to be solved in both regions. After this, the solutions for both areas have to be coupled by transmission conditions at the solid liquid interface.

2.1. Solid region (wall)

Fig. 2 shows the solid wall, together with the local coordinate system x_1, y_1 and the boundary conditions. Assuming steady-state conditions and constant properties of the wall, the energy equation for this region simplifies to

$$\frac{\partial^2 T}{\partial x_1^2} + \frac{\partial^2 T}{\partial y_1^2} = 0 \tag{1}$$

Eq. (1) has to be solved together with the following boundary conditions

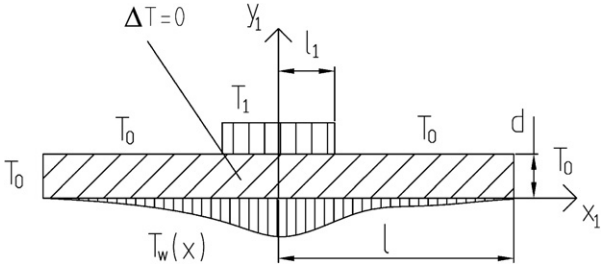

Fig. 2. Boundary conditions for the solid region.

$$\begin{aligned} &x_1 = \pm l: \ T = T_0 \\ &y_1 = 0: \ T = T_W(x_1) \\ &y_1 = d: \ T = T_0, \quad x_1 < l_1 \quad \text{and} \quad x_1 > l \\ &T = T_1, \quad -l_1 \leqslant x_1 \leqslant l_1 \end{aligned} \tag{2}$$

It has to be noted here that the wall temperature $T_W(x_1)$ is yet unknown. Furthermore, it is clear, that the length l has to be taken to be very large and tends to infinity. However, the temperature solution for the solid region has been developed here for a finite length l in order to be able to study the length effect on the convergence and the accuracy of the solution and also in order to compare the obtained analytical solution later easier to numerical results from FLUENT, where a finite length of the channel had to be used anyway. The solution of Eq. (1), with the boundary conditions according to Eq. (2), can be obtained by using the method of separation of variables. For this, it is useful to construct the solution of two parts, one is the temperature jump at the outer wall, and one is the variable inner surface temperature. The variable inner surface temperature has been represented by a Fourier series expression, given by Eq. (6). After doing so, one finally obtains:

$$\begin{aligned} \Theta_s = &\sum_{j=0}^{\infty} \frac{a_j}{\sinh(\psi_j \tilde{d}\tilde{h})} \cos(\psi_j \tilde{d}\tilde{h}\bar{x}) \sinh(\psi_j \tilde{h}\tilde{d}\bar{y}) \\ &+ \sum_{j=0}^{\infty} \frac{b_j}{\sinh(-\psi_j \tilde{d}\tilde{h})} \cos(\psi_j \tilde{d}\tilde{h}\bar{x}) \sinh(\psi_j \tilde{d}\tilde{h}(\bar{y}-1)) \\ &+ \sum_{j=0}^{\infty} \frac{c_j}{\sinh(-\varphi_j \tilde{d}\tilde{h})} \sin(\varphi_j \tilde{d}\tilde{h}\bar{x}) \sinh(\varphi_j \tilde{d}\tilde{h}(\bar{y}-1)) \end{aligned} \tag{3}$$

where the definitions

$$\begin{aligned} &\Theta_s = \frac{T - T_0}{T_1 - T_0}, \quad \bar{x} = \frac{x_1}{d}, \quad \bar{y} = \frac{y_1}{d}, \quad \tilde{l}_1 = \frac{l_1}{l}, \\ &\tilde{l} = \frac{l}{d}, \quad \tilde{d} = \frac{d}{h}, \quad \tilde{h} = \frac{h}{l}, \\ &\varphi_j = \pi(j+1), \quad \psi_j = \pi(2j+1)/2 \end{aligned} \tag{4}$$

have been used. The constants a_j are given by

$$a_j = \frac{2}{\psi_j} \sin(\psi_j \tilde{l}_1) \tag{5}$$

The constants b_j, c_j, which appear in Eq. (3), will determine the unknown wall temperature distribution at the inner wall, given by

$$\begin{aligned} \Theta_{sW}(\bar{x}) = \Theta_s(\bar{x}, 0) &= \frac{T_W - T_0}{T_1 - T_0} \\ &= \sum_{j=0}^{\infty} b_j \cos(\psi_j \tilde{d}\tilde{h}\bar{x}) + c_j \sin(\varphi_j \tilde{d}\tilde{h}\bar{x}) \end{aligned} \tag{6}$$

These constants have to be determined later by the transmission conditions at the solid fluid interface.

2.2. Liquid region (fluid)

Under the assumptions of an incompressible flow with constant fluid properties, negligible viscous and turbulent

energy dissipation and hydrodynamically fully-developed flow, the energy equation is given by

$$\rho c_p u(y)\frac{\partial T}{\partial x} = \frac{\partial}{\partial y}\left[\left(k+\rho c_p\frac{\varepsilon_m}{Pr_t}\right)\frac{\partial T}{\partial y}\right] + \frac{\partial}{\partial x}\left[\left(k+\rho c_p\frac{\varepsilon_m}{Pr_t}\frac{\varepsilon_{hx}}{\varepsilon_{hy}}\right)\frac{\partial T}{\partial x}\right] \tag{7}$$

with the boundary conditions

$$\begin{aligned} &x\to\infty:\ T=T_0,\quad x\to-\infty:\ T=T_0\\ &y=0:\ \frac{\partial T}{\partial y}=0\\ &y=h:\ T=T_{\mathrm{W}}(x)\end{aligned} \tag{8}$$

The velocity distribution u in Eq. (7), has been calculated from the momentum equation for hydrodynamically fully-developed flow. For a turbulent flow, the turbulent shear stress has been approximated using a mixing length model. The reader is referred to Weigand [8] for more details. By introducing the following dimensionless quantities:

$$\begin{aligned} &\Theta=\frac{T-T_0}{T_1-T_0},\quad \tilde{x}=\frac{x}{h}\frac{1}{Pe_{\mathrm{h}}},\quad \tilde{u}=\frac{u}{\bar{u}_0},\quad \tilde{y}=\frac{y}{h},\\ &Pe_{\mathrm{h}}=Re_{\mathrm{h}}Pr,\quad Re_{\mathrm{h}}=\frac{\bar{u}_0 h}{\nu},\quad Pr=\frac{\nu}{a},\quad \tilde{\varepsilon}_m=\frac{\varepsilon_m}{\nu},\quad Pr_t=\frac{\varepsilon_m}{\varepsilon_{hy}}\end{aligned} \tag{9}$$

where $\bar{u}_0$ denotes the axial mean velocity at the entrance of the channel, into Eqs. (7) and (8), the energy equation can be cast into the following non-dimensional form:

$$\tilde{u}(\tilde{y})\frac{\partial\Theta}{\partial\tilde{x}} = \frac{1}{Pe_{\mathrm{h}}^2}\frac{\partial}{\partial\tilde{x}}\left[a_1(\tilde{y})\frac{\partial\Theta}{\partial\tilde{x}}\right]+\frac{\partial}{\partial\tilde{y}}\left[a_2(\tilde{y})\frac{\partial\Theta}{\partial\tilde{y}}\right] \tag{10}$$

with the boundary conditions

$$\begin{aligned} &\tilde{y}=1:\ \Theta=\Theta_{sW}(\tilde{x})\\ &\tilde{y}=0:\ \frac{\partial\Theta}{\partial\tilde{y}}=0\\ &\lim_{\tilde{x}\to-\infty}\Theta=0,\quad \lim_{\tilde{x}\to+\infty}\Theta=0\end{aligned} \tag{11}$$

The functions $a_1(\tilde{y})$and $a_2(\tilde{y})$ are given by

$$a_1(\tilde{y}) = 1+\frac{Pr}{Pr_t}\tilde{\varepsilon}_m\left(\frac{\varepsilon_{hx}}{\varepsilon_{hy}}\right) \tag{12}$$

$$a_2(\tilde{y}) = 1+\frac{Pr}{Pr_t}\tilde{\varepsilon}_m \tag{13}$$

In the following solution process for Eq. (10) no assumptions are required about the functions $a_1(\tilde{y})$ and $a_2(\tilde{y})$. The solution presented here holds for arbitrary functions $a_1(\tilde{y})$ and $a_2(\tilde{y})$ as long as $a_1\geqslant 1, a_2\geqslant 1$ which is obviously true from the structure of Eqs. (12) and (13). Therefore, the turbulent Prandtl number as well as the ratio $\varepsilon_{hx}/\varepsilon_{hy}$, used in Eqs. (12) and (13), will be specified later. Papoutsakis et al. [5] showed that it is possible to solve Eq. (10) for laminar pipe flow ($a_1=a_2=1$) by decomposing the elliptic partial differential equation into a pair of first order partial differential equations. For turbulent flows this has been shown later (Weigand [8]) by using a different inner product between two vectors. Weigand and Lauffer [11] derived a solution for the energy equation for a piecewise constant wall temperature distribution. The ensuing procedure for solving the problem here considered follows the method given by [5,8,11] for deriving the solution of the more general problem, considered here. Let us define a function $\Sigma(\tilde{x},\tilde{y})$, which may be called the axial energy flow through a cross-sectional area of the height $\tilde{y}$ by

$$\Sigma(\tilde{x},\tilde{y}) = \int_0^{\tilde{y}}\left[\tilde{u}\Theta-\frac{1}{Pe_{\mathrm{h}}^2}a_1(\hat{y})\frac{\partial\Theta}{\partial\tilde{x}}\right]\mathrm{d}\hat{y}. \tag{14}$$

Introducing Σ, defined by Eq. (14), into the energy equation (10) results in the following system of partial differential equations:

$$\frac{\partial}{\partial\tilde{x}}\vec{S}(\tilde{x},\tilde{y}) = \underset{\sim}{L}\,\vec{S}(\tilde{x},\tilde{y}) \tag{15}$$

with the two component vector $\vec{S}$ and the operator $\underset{\sim}{L}$ given by

$$\vec{S}=\begin{bmatrix}\Theta(\tilde{x},\tilde{y})\\ \Sigma(\tilde{x},\tilde{y})\end{bmatrix},\quad \underset{\sim}{L}=\begin{bmatrix}\frac{Pe_{\mathrm{h}}^2\tilde{u}}{a_1(\tilde{y})} & -\frac{Pe_{\mathrm{h}}^2}{a_1(\tilde{y})}\frac{\partial}{\partial\tilde{y}}\\ a_2(\tilde{y})\frac{\partial}{\partial\tilde{y}} & 0\end{bmatrix} \tag{16}$$

The boundary conditions belonging to $\Sigma(\tilde{x},\tilde{y})$ can be derived from Eqs. (8) and (14)

$$\tilde{y}=0:\Sigma(\tilde{x},0)=0,\quad \lim_{\tilde{x}\to-\infty}\Sigma=0 \tag{17}$$

Before calculating the solution of Eq. (10), some interesting details about the operator L and the corresponding eigenvalue problem for Eq. (15) should be presented. The most remarkable aspect of L is that it gives rise to a selfadjoint problem even though the original convective diffusion operator is non-selfadjoint. This fact is of course dependent on the sort of inner product between two vectors, which will be used. If we define an inner product between two vectors

$$\vec{\Phi}=\begin{bmatrix}\Phi_1(\tilde{y})\\ \Phi_1(\tilde{y})\end{bmatrix},\quad \vec{\Lambda}=\begin{bmatrix}\Lambda_1(\tilde{y})\\ \Lambda_1(\tilde{y})\end{bmatrix} \tag{18}$$

$$\langle\vec{\Phi},\vec{\Lambda}\rangle = \int_0^1\left[\frac{a_1(\tilde{y})}{Pe_{\mathrm{h}}^2}\Phi_1(\tilde{y})\Lambda_1(\tilde{y})+\frac{1}{a_2(\tilde{y})}\Phi_2(\tilde{y})\Lambda_2(\tilde{y})\right]\mathrm{d}\tilde{y} \tag{19}$$

and the following domain for $(\underset{\sim}{L})$

$$D(\underset{\sim}{L}) = \{\vec{\Phi}\in H:\underset{\sim}{L}\,\vec{\Phi}\ (\text{exists and})\ \in H,\Phi_1(1)=\Phi_2(0)=0\} \tag{20}$$

then it can be shown that is a symmetric operator in the Hilbert space H of interest (this means that $\langle\vec{\Phi},\underset{\sim}{L}\,\vec{\Lambda}\rangle = \langle\underset{\sim}{L}\,\vec{\Phi},\vec{\Lambda}\rangle$). The reader is referred to Weigand [8,3] for more details. Thus the selfadjoint eigenvalue problem associated with Eq. (15) is given by

$$\underset{\sim}{L}\,\vec{\Phi}_j = \lambda_j\vec{\Phi}_j \tag{21}$$

where $\vec{\Phi}_j$ denotes the eigenvector corresponding to the eigenvalue λ_j. Using the definition of the matrix operator L, given by Eq. (16), the eigenvalue problem (21) can be rewritten in the form

$$Pe_h^2\left[\frac{\tilde{u}(\tilde{y})}{a_1(\tilde{y})}\Phi_{j1}-\frac{1}{a_1(\tilde{y})}\Phi'_{j2}\right]=\lambda_j\Phi_{j1} \tag{22}$$

$$a_2(\tilde{y})\Phi'_{j1}=\lambda_j\Phi_{j2} \tag{23}$$

If Φ_{j2} is eliminated from Eq. (22), the following eigenvalue problem for Φ_{j1} can be obtained (see also Weigand [3])

$$[a_2(\tilde{y})\Phi'_{j1}]'+\left[\frac{\lambda_j a_1(\tilde{y})}{Pe_h^2}-\tilde{u}(\tilde{y})\right]\lambda_j\Phi_{j1}=0 \tag{24}$$

Eq. (24) has to be solved in conjunction with the boundary conditions

$$\Phi'_{j1}(0)=0,\quad \Phi_{j1}(1)=0 \tag{25}$$

In addition, an arbitrary normalizing condition

$$\Phi_{j1}(0)=1 \tag{26}$$

will be used. Eq. (24) possesses both, positive eigenvalues λ_j^+ with the corresponding eigenvectors Φ_j^+ and negative eigenvalues λ_j^- with eigenvectors Φ_j^-. This is because the operator is neither positive nor negative definite. All λ_j are real because they are in fact the eigenvalues of a selfadjoint problem. Because the two sets of eigenvectors, normalized according to Eq. (26), constitute an orthogonal basis in H (see [5,8]) an arbitrary vector $\vec{f}$ can be expanded in terms of eigenfunctions in the following way:

$$\vec{f}=\sum_{j=0}^{\infty}\frac{\langle\vec{f},\vec{\Phi}_j\rangle}{\|\vec{\Phi}_j\|^2}\vec{\Phi}_j(\tilde{y}) \tag{27}$$

with the vector norm $\|\vec{\Phi}_j\|^2=\langle\vec{\Phi}_j,\vec{\Phi}_j\rangle$. If we explicitly distinguish in Eq. (27) between positive and negative eigenvectors, Eq. (27) takes the following form:

$$\vec{f}=\sum_{j=0}^{\infty}\frac{\langle\vec{f},\vec{\Phi}_j^+\rangle}{\|\vec{\Phi}_j^+\|^2}\vec{\Phi}_j^+(\tilde{y})+\sum_{j=0}^{\infty}\frac{\langle\vec{f},\vec{\Phi}_j^-\rangle}{\|\vec{\Phi}_j^-\|^2}\vec{\Phi}_j^-(\tilde{y}) \tag{28}$$

Now the solution of Eq. (15) can be reconsidered. The solution of the problem $\vec{S}(\tilde{x},\tilde{y})$ will be obtained in the form of the series given by Eq. (28). Therefore, the inner product appearing in the expansion coefficients of Eq. (28) must be determined. It can be shown [5,10,13] that

$$\langle\underset{\sim}{L}\vec{S},\vec{\Phi}_j\rangle=\langle\vec{S},\underset{\sim}{L}\vec{\Phi}_j\rangle+\Phi_{j2}(1)g(\tilde{x}) \tag{29}$$

The function $g(\tilde{x})$ is in the present study given by (see also Eq. (6))

$$\text{for } |\tilde{x}|\leqslant\frac{1}{\tilde{h}Pe_h}:\ g(\tilde{x})=\Theta_{sW}(\tilde{x})=\sum_{i=0}^{\infty}b_i\cos(\psi_i\tilde{h}Pe_h\tilde{x})+c_i\sin(\varphi_i\tilde{h}Pe_h\tilde{x})$$

$$\text{for } |\tilde{x}|\geqslant\frac{1}{\tilde{h}Pe_h}:\ g(\tilde{x})=0 \tag{30}$$

This means that we always assume that the function $g(\tilde{x})$ tends to zero for large $|\tilde{x}|$. This means that the ratio l_1/l is assumed to be large. Taking the inner product of both sides of Eq. (15) with $\vec{\Phi}_j$ and using Eq. (29) one obtains

$$\frac{\partial}{\partial\tilde{x}}\langle\vec{S},\vec{\Phi}_j\rangle=\lambda_j\langle\vec{S},\vec{\Phi}_j\rangle+g(\tilde{x})\Phi_{j2}(1) \tag{31}$$

Eq. (31) can be solved separately for positive and negative eigenvalues. This results in

$$\langle\vec{S},\vec{\Phi}_j^-\rangle=C_{0j}^-\exp(\lambda_j^-\tilde{x})+\int_{-\infty}^{\tilde{x}}(g(\hat{x})\Phi_{j2}^-(1))\exp(\lambda_j^-(\tilde{x}-\hat{x}))\,\mathrm{d}\hat{x} \tag{32}$$

$$\langle\vec{S},\vec{\Phi}_j^+\rangle=C_{0j}^+\exp(\lambda_j^+\tilde{x})-\int_{\tilde{x}}^{\infty}(g(\hat{x})\Phi_{j2}^+(1))\exp(\lambda_j^+(\tilde{x}-\hat{x}))\,\mathrm{d}\hat{x} \tag{33}$$

Because the solution must be bounded for $\tilde{x}\to+\infty$ and for $\tilde{x}\to-\infty$, the two constants C_0j^- and C_0j^+, appearing in Eqs. (32) and (33) must be zero. In addition, it is assumed that the function $g(\tilde{x})$ tends also to zero for large $|\tilde{x}|$. After carrying out the integrations in Eqs. (32) and (33) the following results for $\Theta(\tilde{x},\tilde{y})$, which is the first vector component of $\vec{S}(\tilde{x},\tilde{y})$, can be derived

$$\begin{aligned}\Theta(\tilde{x},\tilde{y})=&\sum_{j=0}^{\infty}b_j\cos(\bar{\psi}_j\tilde{x})\left[\sum_{i=1}^{\infty}\frac{\Phi_{i2}^-}{\|\vec{\Phi}_i^-\|^2}\frac{(\bar{\psi}_j)^2\Phi_{i1}^-(\tilde{y})}{((\lambda_i^-)^2+(\bar{\psi}_j)^2)\lambda_i^-}\right.\\&\left.+\sum_{i=1}^{\infty}\frac{\Phi_{i2}^+}{\|\vec{\Phi}_i^+\|^2}\frac{(\bar{\psi}_j)^2\Phi_{i1}^+(\tilde{y})}{((\lambda_i^+)^2+(\bar{\psi}_j)^2)\lambda_i^+}\right]\\&+b_j\sin(\bar{\psi}_j\tilde{x})\left[\sum_{i=1}^{\infty}\frac{\Phi_{i2}^-}{\|\vec{\Phi}_i^-\|^2}\frac{\bar{\psi}_j\Phi_{i1}^-(\tilde{y})}{(\lambda_i^-)^2+(\bar{\psi}_j)^2}\right.\\&\left.+\sum_{i=1}^{\infty}\frac{\Phi_{i2}^+}{\|\vec{\Phi}_i^+\|^2}\frac{\bar{\psi}_j\Phi_{i1}^+(\tilde{y})}{(\lambda_i^+)^2+(\bar{\psi}_j)^2}\right]\\&+c_j\sin(\bar{\varphi}_j\tilde{x})\left[\sum_{i=1}^{\infty}\frac{\Phi_{i2}^-}{\|\vec{\Phi}_i^-\|^2}\frac{(\varphi_j)^2\Phi_{i1}^-(\tilde{y})}{((\lambda_i^-)^2+(\varphi_j)^2)\lambda_i^-}\right.\\&\left.+\sum_{i=1}^{\infty}\frac{\Phi_{i2}^+}{\|\vec{\Phi}_i^+\|^2}\frac{(\varphi_j)^2\Phi_{i1}^+(\tilde{y})}{((\lambda_i^+)^2+(\varphi_j)^2)\lambda_i^+}\right]\\&-c_j\sin(\bar{\varphi}_j\tilde{x})\left[\sum_{i=1}^{\infty}\frac{\Phi_{i2}^-}{\|\vec{\Phi}_i^-\|^2}\frac{\varphi_j\Phi_{i1}^-(\tilde{y})}{(\lambda_i^-)^2+(\varphi_j)^2}\right.\\&\left.+\sum_{i=1}^{\infty}\frac{\Phi_{i2}^+}{\|\vec{\Phi}_i^+\|^2}\frac{\varphi_j\Phi_{i1}^+(\tilde{y})}{(\lambda_i^+)^2+(\varphi_j)^2}\right]\\&+\sum_{j=0}^{\infty}b_j\cos(\bar{\psi}_j\tilde{x})+c_j\sin(\bar{\varphi}_j\tilde{x})\end{aligned} \tag{34}$$

In Eq. (34) the following abbreviations have been used:

$$\bar{\psi}_j=\psi_j\tilde{h}Pe_h,\quad \bar{\varphi}_j=\varphi_j\tilde{h}Pe_h \tag{35}$$

From Eq. (34) it is obvious that the temperature distribution in the fluid consists of two parts

$$\Theta(\tilde{x},\tilde{y})=\Theta_h(\tilde{x},\tilde{y})+\Theta_{sW}(\tilde{x}) \tag{36}$$

This means that the temperature distribution consists of a part, which is the solution of the homogeneous problem

and one part, which is a particular solution of the problem. Eq. (34) shows also very nicely that the solution fulfils the boundary condition at the wall, because for $\tilde{y} = 1$, the eigenfunctions Φ_{i1} (1) in the first term on the right hand side of Eq. (34) will vanish and therefore this term is equal to zero.

2.3. Coupling of the temperature solutions for the wall and the flow region

Up to now, the constants b_j and c_j are still unknown. These constants can be obtained by finally coupling the temperature solution for the solid region with the one for the flow area. This can be achieved by satisfying the following coupling conditions:

$$y = h: \quad T_s = T, \quad k_s \frac{\partial T_s}{\partial y} = k \frac{\partial T}{\partial y} \tag{37}$$

The two conditions given by Eq. (37) state that the temperature and the heat flux at the inner wall have to be identical between the fluid and the wall region at the inner surface. By deriving Eq. (34) we already showed that the temperatures in the solid and liquid region are equal at the inner wall. Therefore, only the second condition in Eq. (37) has to be satisfied. This can be done by using Eq. (34) for the fluid region and Eq. (3) for the solid area. Because the sin- and cos-functions appearing in these equations have not the same frequency, they have to be expanded into a Fourier series. This leads finally to a system of linear equations for the unknown coefficients, which has been solved by the CGN method [16].

It should be noted, that the here presented solution method can easily been applied to a large class of similar problems dealing with conjugate heat transfer (e.g. heat transfer in circular tubes, concentric annuli,...).

3. Results and discussion

In order to obtain solutions of the energy equation (7), the turbulent Prandtl number and the ratio $(\varepsilon_{hx}/\varepsilon_{hy})$ appearing in Eqs. (12) and (13) have to be specified. There is a variety of different models in the literature prescribing the turbulent Prandtl number. Especially in the case of liquid metal flows the values for Pr_t given by several models are quite different. A good literature review concerning different models for the turbulent Prandtl number can be found in [17]. For the results presented here the extended Kays and Crawford model [2] was used because this model predicts very well experimental results for the Nusselt numbers for liquid metal flows. The reader is referred to [2] for more details. The model for the turbulent Prandtl number is given by

$$Pr_t = \left(\frac{1}{2Pr_{t\infty}} + CPe_t \sqrt{\frac{1}{Pr_{t\infty}}} - (CPe_t)^2 \left[1 - \exp\left(-\frac{1}{CPe_t \sqrt{Pr_{t\infty}}} \right) \right] \right)^{-1} \tag{38}$$

with the quantities

$$Pe_t = \tilde{\varepsilon}_m Pr, \quad C = 0.3, \quad Pr_{t\infty} = 0.85 + \frac{100}{PrRe_D^{0.888}} \tag{39}$$

In addition the assumption was made that the ratio of the axial diffusivity to the diffusivity, in y-direction $\varepsilon_{hx}/\varepsilon_{hy}$ appearing in Eq. (12), is equal to one. This assumption has been proven to be correct for the range of parameters here considered. The reader is referred to Weigand et al. [9] for more detailed information on this subject.

3.1. Numerical procedure and accuracy of the predictions

The eigenvalues λ_j as well as the eigenfunctions $\Phi_j(\tilde{y})$ were calculated numerically for the eigenvalue problem given by Eq. (24) by using a four-stage Runge–Kutta scheme. In order to examine the accuracy of the calculated values several calculations were carried out for laminar flows. The eigenvalues calculated here are in very good agreement with those of Deavours [6] for laminar flow in a parallel plate channel. For turbulent flow, the eigenvalues and constants coincide with those reported by Weigand [8]. The first 200 coefficients b_j and c_j determined by the transmission conditions are shown in Figs. 3 and 4. It can be seen, that the coefficients converge rapidly with increasing values of j. In addition, it is obvious that the series converge slower for smaller $\tilde{d} = d/h$. This is due to the increasing temperature gradient in the thinner wall with decreasing values of $\tilde{d}$. For the following calculations normally 200 terms of the sums have been considered. This guarantees a accurate prediction of the temperature field.

3.2. Laminar flow

The heat conduction within the solid wall changes the temperature distribution at the interface between the solid and the fluid. As Fig. 5 shows for $Pe_D = 5$ increasing values of the wall thickness $\tilde{d}$ lead to flatter wall temperature

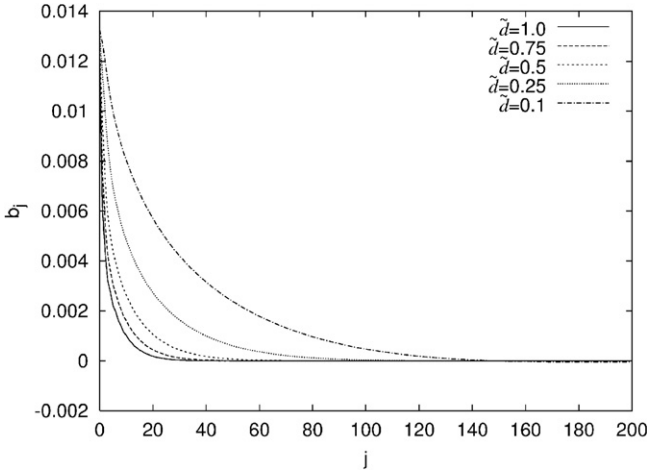

Fig. 3. Distribution of the coefficients b_j for various d/h.

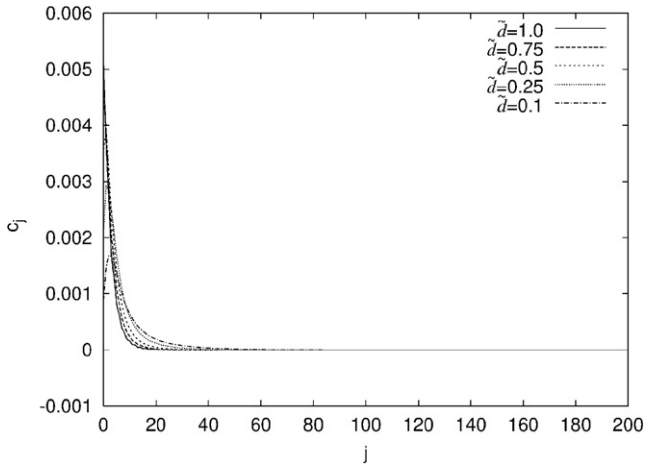

Fig. 4. Distribution of the coefficients c_j for various d/h.

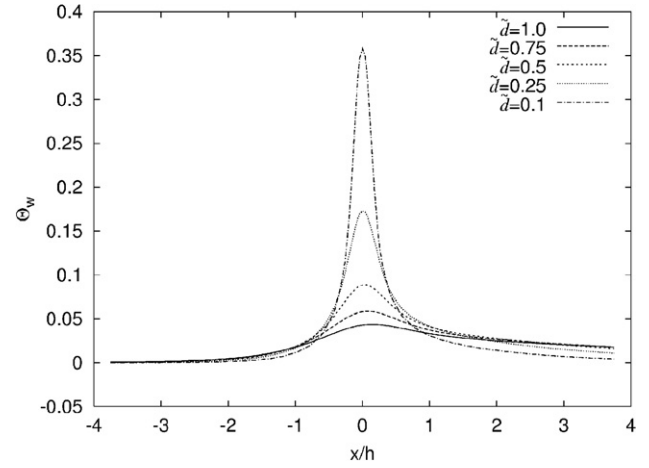

Fig. 5. Axial distribution of the wall temperature inside the parallel plate channel for laminar flow and various d/h.

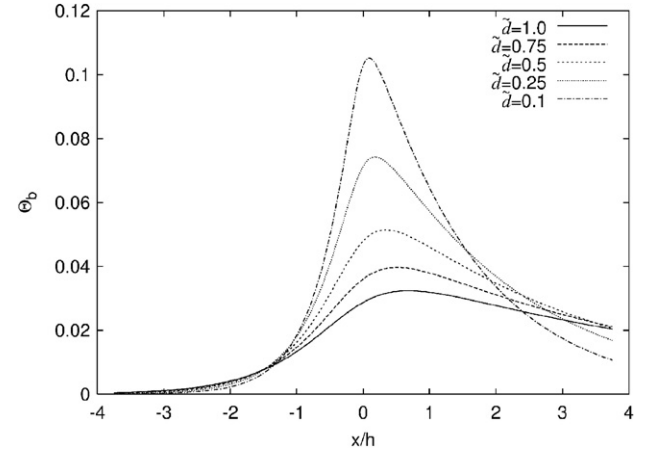

Fig. 6. Axial distribution of the bulk–temperature for laminar flow and various d/h.

distributions. For the same configuration, Fig. 6 depicts the distribution of the bulk–temperature in the fluid defined by

$$T_{\mathrm{b}} = \int_0^h \rho u T \,\mathrm{d}y \Big/ \int_0^h \rho u \,\mathrm{d}y \tag{40}$$

or in dimensionless form

$$\Theta_{\mathrm{b}} = \int_0^1 \tilde{u}(\tilde{y})\Theta(\tilde{x},\tilde{y})\,\mathrm{d}\tilde{y} \tag{41}$$

From Fig. 6 it is obvious that a thicker wall smoothes the temperature jump, which is applied at the outer wall.

3.3. Turbulent flow

Fig. 7 shows the distribution of the non-dimensional bulk–temperature for $Re_{\mathrm{D}} = 5000$ and $Pr = 0.005$. Comparing Fig. 7 to Fig. 6, it can be seen that the temperature gradients in the fluid are steeper in axial direction for turbulent flows. This is obvious, because of the better mixing in the turbulent flow. This is further elucidated in Fig. 8. Here the bulk–temperature distribution is depicted for $l_1/l = 500$ for various Reynolds numbers and a fixed value of the Prandtl number $Pr = 0.005$. It can be seen how the

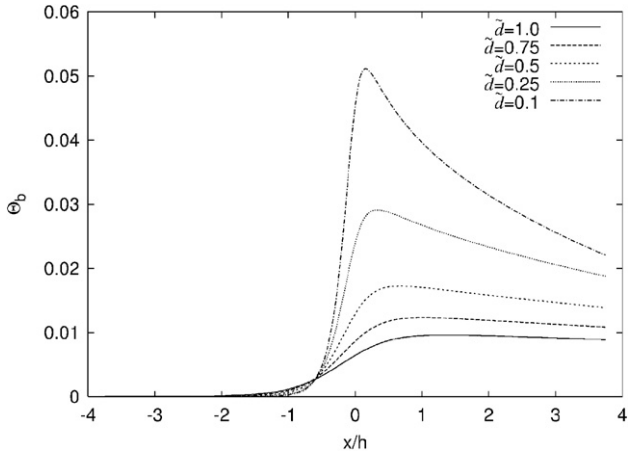

Fig. 7. Axial distribution of the bulk–temperature for turbulent flow ($Re_{\mathrm{D}} = 5000, Pr = 0.05$) for various d/h.

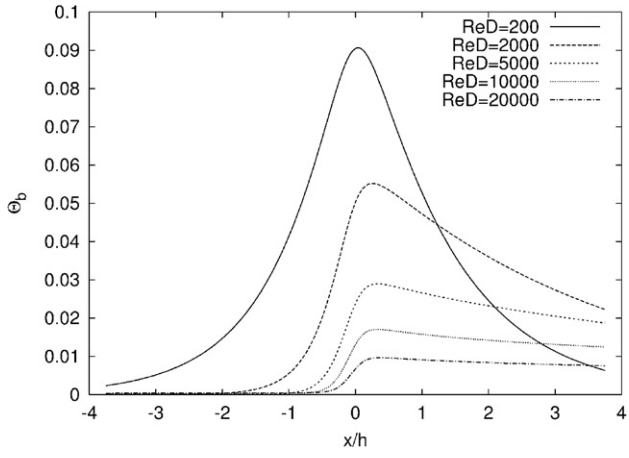

Fig. 8. Axial distribution of the bulk–temperature for turbulent flow, $Pr = 0.05$, and various Reynolds numbers.

axial heat conduction effects in the flow field diminishes for increasing values of the Reynolds and therefore Péclet ($Pe_D = Re_D Pr$) number.

3.4. Comparison with a numerical calculation

For laminar flow, $Re_D = 1000$ and $Pr = 0.005$, the analytical calculation was compared to FLUENT predictions. The used geometry was given by $\tilde{d} = 0.25$ and $l_1/l = 200$. For the FLUENT calculations a structured grid with about 200,000 cells has been used. Fig. 9 shows a comparison between analytically and numerically predicted non-dimensional wall temperature distributions at the inner surface. The prediction of the analytical model needed around one minute on a PC, whereas the numerical calculation with FLUENT took some hours on a SUN ULTRA 60 workstation. It can be seen that the numerically predicted wall temperature distribution with FLUENT is generally in good agreement with the analytically obtained wall temperature. However, near the sharpest axial temperature gradients, the numerical calculation shows some deviations. This might be caused by insufficient grid resolution in the numerical prediction in this area.

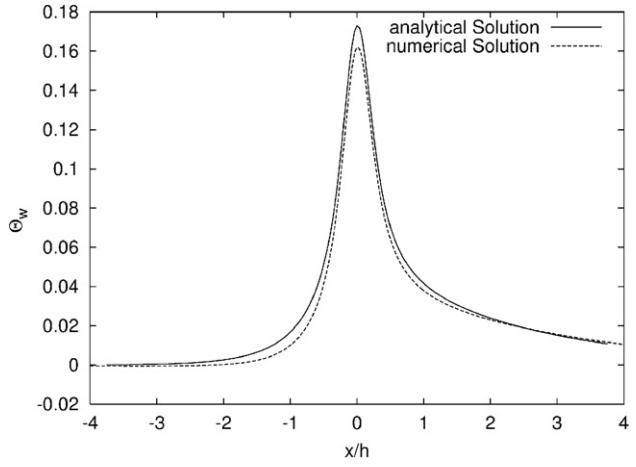

Fig. 9. Comparison between the numerically calculated and analytically predicted wall temperature distribution inside the channel.

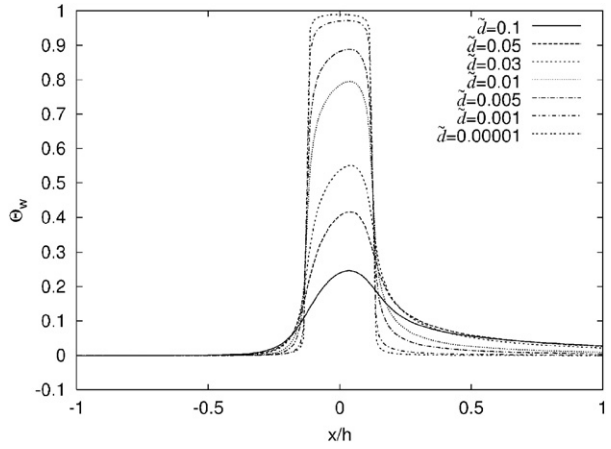

Fig. 10. Wall temperature distribution at the inner wall for various values of the wall thickness.

If the wall thickness $\tilde{d} \to 0$, the non-dimensional temperature distribution at the inner wall of the channel should converge to the temperature jump boundary condition, which has been applied at the outer channel wall. This has been tested for $Re_D = 1000$, $Pr = 0.005$, $l_1/l = 200$. The results are shown in Fig. 10 for various values of the dimensionless wall thickness $\tilde{d} = d/h$. This might be considered as a further validation of the analytical solution.

4. Conclusions

According to the present analytical study concerning the influence of axial heat conduction within the fluid and the solid, the following major conclusions can be drawn:

Axial heat conduction effects in the fluid are important for low Péclet numbers. However, if short heating sections are considered, these effects might drastically influence the heat transfer behaviour even for higher Péclet numbers.

The analytical predictions agree well with own numerical calculations using FLUENT.

The solution here presented is relatively simple and efficient to compute.

Acknowledgements

The authors would like to acknowledge Dr. A. Haasenritter for carrying out the numerical calculation with FLUENT.

References

[1] R.K. Shah, A.L. London, Laminar Flow Forced Convection in Ducts, Chapters V and VI, Academic Press, New York, 1978.
[2] W.M. Kays, M.E. Crawford, B. Weigand, Convective Heat and Mass Transfer, McGraw-Hill, Inc., New York, 2004.
[3] B. Weigand, Analytical Methods for Heat Transfer and Fluid Flow Problems, Springer, Heidelberg, 2004.
[4] C.J. Hsu, An exact analysis of low Péclet number thermal entry region heat transfer in transversally nonuniform velocity fields, AICHE J. 17 (1971) 732–740.
[5] E. Papoutsakis, D. Ramkrishna, H.C. Lim, The extended Graetz problem with Dirichlet wall boundary conditions, Appl. Sci. Res. 36 (1980) 13–34.
[6] C.A. Deavours, An exact solution for the temperature distribution in parallel plate Poiseuille flow, J. Heat Transfer 96 (1974) 489–495.
[7] S.L. Lee, Forced convection heat transfer in low Prandtl number turbulent flows: influence of axial conduction, Can. J. Chem. Eng. 60 (1982) 482–486.
[8] B. Weigand, An exact analytical solution for the extended turbulent Graetz problem with Dirichlet wall boundary conditions for pipe and channel flows, Int. J. Heat Mass Transfer 39 (1996) 1625–1637.
[9] B. Weigand, T. Schwartzkopff, T.P. Sommer, A numerical investigation of the heat transfer in a parallel plate channel with piecewise constant wall temperature boundary conditions, J. Heat Transfer 124 (2002) 626–634.
[10] B. Weigand, M. Kanzamar, H. Beer, The extended Graetz problem with piecewise constant wall heat flux for pipe and channel flows, Int. J. Heat Mass Transfer 44 (2001) 3941–3952.

[11] B. Weigand, D. Lauffer, The extended Graetz problem with piecewise constant wall temperature for pipe and channel flows, Int. J. Heat Mass Transfer 47 (2004) 5303–5312.
[12] S. Mori, M. Sakakibara, A. Tanimoto, Steady heat transfer to laminar flow in a circular tube with conduction in the wall, Heat Transfer – Jan. Res. 3 (1974) 37–46.
[13] S. Mori, T. Shinke, M. Sakakibara, A. Tanimoto, Steady heat transfer to laminar flow between parallel plates with conduction in the wall, Heat Transfer – Jan. Res. 5 (1976) 17–25.
[14] R.O.C. Guedes, M.N. Özisik, Conjugated turbulent heat transfer with axial conduction in wall and convective boundary conditions in a parallel plate channel, Int. J. Heat Fluid Flow 13 (1992) 322–328.
[15] X. Yin, H.H. Bau, The conjugate Graetz problem with axial heat conduction, ASME J. Heat Transfer 118 (1996) 482–485.
[16] A. Meister, Numerik linearer Gleichungssysteme, Vieweg, 1999.
[17] A.J. Reynolds, The prediction of turbulent Prandtl and Schmidt numbers, Int. J. Heat Mass Transfer 18 (1975) 1055–1069.